Available online at www.sciencedirect.com

ScienceDirect

Journal of the Franklin Institute 360 (2023) 6953–6975

www.elsevier.com/locate/jfranklin

High-order fully actuated system approaches: Model predictive control with applications to under-actuated systems☆

Xiubo Wang[a], Guangren Duan[a,b,*]

[a] *Center for Control Theory and Guidance Technology, Harbin Institute of Technology, Harbin, 150001, China*
[b] *Center for Control Science and Technology, Southern University of Science and Technology, Shenzhen, 518055, China*

Received 19 February 2022; received in revised form 9 March 2023; accepted 10 May 2023
Available online 15 May 2023

Abstract

The main results of this paper are concentrated on the nonlinear model predictive control (MPC) tracking optimization based on high-order fully actuated (HOFA) system approaches. The proposed HOFA MPC strategy makes full use of full-actuation property to eliminate the nonlinear dynamics of the system, and then the nonlinear optimization problem is equivalently transformed into a series of easy-solve linear convex optimization problems. Different from general nonlinear MPC methods and the current optimal control of the HOFA system approach, an analytical controller with smooth and less energy is obtained by the moving horizon optimization. And it is proven that the proposed controller can stabilize the corresponding tracking error closed-loop system. Finally, not limited to FA systems, as examples, a nonlinear numerical under-actuated model in the mathematical sense and a benchmark nonlinear under-actuated mechanical system are transformed into corresponding equivalent HOFA systems, the simulation results are given to verify the effectiveness of the proposed strategy.

☆ This document is the results of the research project funded by the Science Center Program of National Natural Science Foundation of China (62188101), the Major Program of National Natural Science Foundation of China (61690210, 61690212), the National Natural Science Foundation of China (61333003) and the Self-Planned Task of State Key Laboratory of Robotics and System (HIT) (SKLRS201716A).

* Corresponding author.
E-mail address: g.r.duan@hit.edu.cn (G. Duan).

https://doi.org/10.1016/j.jfranklin.2023.05.009

1. Introduction

Full-actuation is originally a fundamental physical property for fully-actuated (FA) robots, which means that each degree of freedom (DOF) of the robots can be directly controlled. This excellent property is generalized systematically, a new approach called the high-order fully actuated (HOFA) system approach is proposed in 2020, which is parallel to the state space method and regarded as a methodology in the control field [1].

The HOFA system approach is applicable to most nonlinear systems. Particularly, in a fully-actuated system (FAS), due to the full-actuation property, the nonlinear dynamics of the open-loop system can be eliminated, and a new desired closed-loop dynamic characteristic can be established. Different from the state-space method, which transforms the system model into the first-order state-space model through the state augmentation, the HOFA system approach retains or constructs the form of FA or HOFA models, which reflects the physical backgrounds [2]. And FASs are widespread because of the configurations of FA actuators and the dominance of a number of physical laws, such as Lagrangian Equation or Theorem of Momentum. Recently, some practical applications have gradually appeared, such as [3–7]. Meanwhile, some benchmark under-actuated systems can also be transformed into HOFA models, such that the corresponding control problems can be easily solved. See, for instance [8–10].

The comprehensive ability of the HOFA system approach is very powerful. By fully utilizing the linear system theory, a series of typical nonlinear control problems can be easily solved by the HOFA system approach, such as robust adaptive control [11], disturbance attenuation and decoupling [12], optimal control [13], generalized PID control and model reference tracking control [14]. Recently, some novel works about the HOFA system approach are dedicated to sub-FASs [15], nonlinear systems with time-delays [16,17], and time-varying [18].

For the nonlinear optimization problem in the frame of the HOFA system approach remains to be enriched. In recent years, as a type of optimal control, model predictive control (MPC) has a great attraction because of the major advantages in dealing with optimization problems in nonlinear optimizations and constrained optimizations. It originates in the industrial field aiming to solve the multi-variable optimization problem numerically online, which can reduce the complexity of calculating the optimal solution based on the Hamilton-Jacobin-equation. There are a lot of work are dedicated to nonlinear MPC for deterministic systems, such as linearized MPC use approximated linear models for optimazition [19]. Dual MPC uses a combination of internal and external-model controllers to obtain suboptimal solutions [20]. Hybrid MPC solves open-loop online optimization and closed-loop optimization in [21]. And distributed MPC considers distributed optimization problems in [22,23]. Economic MPC presents a distributed controller to optimize fuel consumption by combining the switching feedback control [24]. And explicit MPC is computed off-line by using a multi-parametric quadratic programming approximation of the nonlinear problem [25]. Further, many MPC methods are proposed to deal with control of uncertain systems subject to disturbances, constraints of states and control inputs. For examples, [26,27] take multiple disturbances into account. Robust adaptive MPC is used as a comprehensive method to analyze and design the nonlinear system with uncertainties and modeling errors [28,29]. Self-triggered MPC approach absorbs finite-time control to achieve a desired performance [30]. Meanwhile, those methods have been applied to numerous systems, such as linear parameter varying systems [28], time-varying systems [31], time-delay systems [32], Markov jump linear systems and

stochastic systems [30]. Various algorithms are presented derived from branches of learning strategies [33,34].

In recent years, these MPC methods have been rapidly applied in physical systems, such as autonomous driving fields [35], hydraulic servo actuators [36], aerospace industries [37] and smart energy grid projects [38,39]. More details can be found in [40,41] and the references therein. It should be noteworthy that in dealing with the disturbances, modeling errors, various uncertainties, except for MPC, the control methods based on driven control, such as [42,43] also have excellent performance. And the optimization involving nonlinear elimination and multi-variables decoupling from the proposed method in this paper can be further extended to the above mentioned related problems, such that the applicable range of application objects can be wider, and the control optimization problem may become simpler. But in this paper, our research is only concentrate on the aspect of nonlinear optimization for the deterministic system, the uncertainties are not considered in this paper.

The major difficulties encountered in this paper are the nonlinear optimization design for the nonlinear system with strongly nonlinear, coupling between multi-variables of mix-order, even time-delay or time-varying, simultaneously. As the general nonlinear MPC methods, these multi-variable mix-order systems are converted into first-order state spaces through variable augmentation, and it does not appear easy to get an explicit analytical optimal solution. Although a numerical optimal solution can be obtained by many online optimization algorithms, the existence of optimal solution does not mean that the corresponding closed-loop system is stable. The nonlinear dynamics also need to be tackled with Lyapunov stability design approaches. For the stability analysis, it is very difficult to find the appropriate Lyapunov function for the augmented first-order system, not to mention that the system contains time-varying or delay factors.

Aiming at the above observations and discussions, in this paper, we dedicate to promoting a new nonlinear optimization in the unified framework of the HOFA system approaches along the MPC field. And the main contributions of this work are given as follows:

1. A nonlinear system optimization problem that simultaneously contains complex nonlinearities, strong coupling, and time-varying or delay factors is solved by MPC based on the HOFA system approach. According to the proposed strategy, the predictive states are depicted by the information of the constructed HOFA system in the compact linear form. And a complex nonlinear optimization problem is equivalently decomposed into a series of easy-solve linear convex optimization ones.
2. Different from the existing nonlinear MPC methods, an analytical explicit optimal controller is obtained in this paper. Firstly, in the optimization process, the mixed-order form of the original system which may have a physics background, is preserved. Secondly, a fixed-form controller is set to eliminate the nonlinearities in the system, such that response of the controller is smoother and achieves steady transient performance. Compared with the existing optimal control method based on HOFA system approaches, the proposed controller obtained by the moving horizon optimization owns fast disturbance recovery capability and requires less control energy.
3. Not limited to nonlinear HOFA systems, as examples, a numerical nonlinear under-actuated model in the mathematical sense and a benchmark nonlinear under-actuated mechanical system are transformed into corresponding equivalent HOFA systems by model conversion. The variable redundancy relationship in the system can be seen intuitively, which brings conveniences to the control of the FA systems and under-actuated FA systems in practice.

The remaining contents are organized as follows. The expositions of the HOFA system and the formulation of the HOFA-MPC problem are given in Section 2. Section 3 exploits the design of the HOFA-MPC, and the proof of the stability of the corresponding tracking error closed-loop system is given. The proposed scheme of HOFA-MPC is applied to under-actuated nonlinear systems to demonstrate the effectiveness of the proposed method in Section 4. Finally, a brief conclusion is presented in Section 5.

For the sake of convenience, the following notations are frequently used in this paper. For $x,\ x_k \in \mathbb{R}^m,\ k,\ i,\ j \in \mathbb{N},\ i \le j$, the following symbols are used:

$$x^{(0\sim n)} = \begin{bmatrix} x^{\mathrm{T}} & \dot{x}^{\mathrm{T}} & \cdots & \left(x^{(n)}\right)^{\mathrm{T}} \end{bmatrix}^{\mathrm{T}},$$

$$x_k|_{k=i\sim j} = \begin{bmatrix} x_i^{\mathrm{T}} & x_{i+1}^{\mathrm{T}} & \cdots & x_j^{\mathrm{T}} \end{bmatrix}^{\mathrm{T}},\ i \le j,$$

$$x_k^{(0\sim n)}|_{k=i\sim j} = \begin{bmatrix} \left(x_i^{(0\sim n)}\right)^{\mathrm{T}} & \left(x_{i+1}^{(0\sim n)}\right)^{\mathrm{T}} & \cdots & \left(x_j^{(0\sim n)}\right)^{\mathrm{T}} \end{bmatrix}^{\mathrm{T}},\ i \le j,$$

$$x_k^{(n_0\sim n_k)}|_{k=i\sim j} = \begin{bmatrix} \left(x_i^{(n_0\sim n_i)}\right)^{\mathrm{T}} & \left(x_{i+1}^{(n_0\sim n_i+1)}\right)^{\mathrm{T}} & \cdots & \left(x_j^{(n_0\sim n_j)}\right)^{\mathrm{T}} \end{bmatrix}^{\mathrm{T}},\ i \le j.$$

For $A_k \in \mathbb{R}^{m\times m},\ k \in \mathbb{N},$ and $f\left(A_i, A_j\right) \in \mathbb{R}^{m\times m},\ n_i \in \mathbb{N},\ i = 1 \sim 4,$ we denote

$$\Phi(A_{1\sim n}) = \begin{bmatrix} 0 & I_m & & \\ & & \ddots & \\ & & & I_m \\ -A_1 & -A_2 & \cdots & -A_n \end{bmatrix},$$

$$\text{blockdiag}(A_i,\ i = 1 \sim n) = \begin{bmatrix} A_1 & 0 & \cdots & 0 \\ 0 & A_2 & \cdots & 0 \\ \vdots & \vdots & \ddots & \vdots \\ 0 & 0 & \cdots & A_n \end{bmatrix},$$

$$\text{block}\left\{ f\left(A_i, A_j\right), {}^{i=n_1\sim n_2}_{j=n_3\sim n_4} \right\} = \begin{bmatrix} f\left(A_{n_1}, A_{n_3}\right) & f\left(A_{n_1}, A_{n_3+1}\right) & \cdots & f\left(A_{n_1}, A_{n_4}\right) \\ f\left(A_{n_1+1}, A_{n_3}\right) & f\left(A_{n_1+1}, A_{n_3+1}\right) & \cdots & f\left(A_{n_1+1}, A_{n_4}\right) \\ \vdots & \vdots & \ddots & \vdots \\ f\left(A_{n_2}, A_{n_3}\right) & f\left(A_{n_2}, A_{n_3+1}\right) & \cdots & f\left(A_{n_2}, A_{n_4}\right) \end{bmatrix}.$$

2. Preliminaries and problem formulation

We begin with presentations and expositions of HOFA model and the receding-horizon optimization, and give the statement of problem in this paper.

2.1. HOFA Model

Consider the following general continuous-time mix-order nonlinear system proposed in [2]:

$$\begin{bmatrix} x_1^{(\mu_1)}(t) \\ x_2^{(\mu_2)}(t) \\ \vdots \\ x_\eta^{(\mu_\eta)}(t) \end{bmatrix} = \begin{bmatrix} f_1\left(x_k^{(0\sim\mu_k-1)}|_{k=1\sim\eta}(t),\zeta,t\right) \\ f_2\left(x_k^{(0\sim\mu_k-1)}|_{k=1\sim\eta}(t),\zeta,t\right) \\ \vdots \\ f_\eta\left(x_k^{(0\sim\mu_k-1)}|_{k=1\sim\eta}(t),\zeta,t\right) \end{bmatrix} + B\left(x_k^{(0\sim\mu_k-1)}|_{k=1\sim\eta}(t),\zeta,t\right)u(t), \tag{1}$$

where $u \in \mathbb{R}^\gamma$ is the input, $\zeta \in \mathbb{R}^p$ is the external vector which may present a time-delay vector, a time varying vector, etc. For $k = 1, 2, \cdots, \eta$, $x_k \in \mathbb{R}^{r_k}$ are states, and $f_k(\cdot) \in \mathbb{R}^{r_k}$ are a set of nonlinear vector functions. Moreover, μ_k and r_k are sets of integers satisfying

$$\begin{cases} \sum r_k = \gamma \\ \sum r_k\mu_k = \chi. \end{cases} \tag{2}$$

And $B(\cdot) \in \mathbb{R}^{\gamma\times\gamma}$ is the sufficiently differentiable nonlinear matrix function satisfying the following full-actuation condition according to the definition of the HOFA system in [1]:

Assumption 1. $\det B(\cdot) \neq 0$ or ∞, for all $x_k^{(0\sim\mu_k-1)}|_{k=1\sim\eta}$, ζ and $t \geq 0$.

More compactly, the above HOFA model (1) can be transformed into the following form

$$x_k^{(\mu_k)}|_{k=1\sim\eta}(t) = f\left(x_k^{(0\sim\mu_k-1)}|_{k=1\sim\eta}(t),\zeta,t\right) + B\left(x_k^{(0\sim\mu_k-1)}|_{k=1\sim\eta}(t),\zeta,t\right)u(t), \tag{3}$$

where

$$f\left(x_k^{(0\sim\mu_k-1)}|_{k=1\sim\eta}(t),\zeta,t\right) = \begin{bmatrix} f_1\left(x_k^{(0\sim\mu_k-1)}|_{k=1\sim\eta}(t),\zeta,t\right) \\ f_2\left(x_k^{(0\sim\mu_k-1)}|_{k=1\sim\eta}(t),\zeta,t\right) \\ \vdots \\ f_\eta\left(x_k^{(0\sim\mu_k-1)}|_{k=1\sim\eta}(t),\zeta,t\right) \end{bmatrix}.$$

Remark 1. The nonlinear mix-order system (1) with Assumption 1 is a quite compatible and complex system. Due to physical laws, there are many practice systems can directly be modeled in this form [2]. Depending on the choice of μ_k, the system (1) can present a variety of systems, such as first-order FA systems, second-order FA systems, HOFA systems and more general mix-order FA systems. If μ_k are fractions, the system (1) can even represent fractional mix-order systems, which is not considered in this paper. When each subsystem contains complex nonlinear dynamics, strong couplings, and even time delay or time-varying factors.

2.2. Problem formulation

Before the problem formulation, we first give some statements and definitions about the receding-horizon optimization.

For the receding-horizon optimization operation, at each time t, there is a forward moving time period frame for the prediction, and the length of the time period frame is T_p, which

is called the predictive period. To name an example, for $0 < \tau < t + T_p$, $\hat{x}(t+\tau)$ is the state variable with the initial value $x(t)$ in the forward moving time period frame, that is, $\hat{x}(t+\tau) = x_k^{(0\sim\mu_k-1)}|_{k=1\sim\eta}(t)$ when $\tau = 0$.

Definition 1 [44]**.** The control order in the continuous-time predictive control is said to be r if the control signal $\hat{u}(t+\tau)$ satisfies

$$\hat{u}^{(r)}(t+\tau) \neq 0, \text{ for some } \tau \in [0, T],$$

and

$$\hat{u}^{(k)}(t+\tau) = 0, \text{ for all } k > r \text{ and } \tau \in [0, T],$$

where $\hat{u}^{(r)}(t+\tau)$ denotes the r-th derivative of $\hat{u}(t+\tau)$ with respect to τ.

Inspired by the Taylor series expansion, we define all the predictive states variables in the moving period time frame with a truncated Taylor series expansion to ρ-th order in this paper. To take a specific example, the predictive value of the state variable x can be characterized as follows:

$$\hat{x}(t+\tau) \triangleq x(t) + \tau\dot{x}(t) + \cdots + \frac{1}{\rho!}\tau^{\rho}x^{(\rho)}(t), \ 0 < \tau < t + T_p, \tag{4}$$

where the order of truncated Taylor series expansion ρ is named as the predictive order.

Further, to formulate the tracking performance, we introduce the following receding-horizon performance index at each instant t:

$$\begin{aligned} &J\Big(x_k^{(0\sim\mu_k-1)}|_{k=1\sim\eta}(t), r_k^{(0\sim\mu_k-1)}|_{k=1\sim\eta}(t), T_P, \rho, m, t\Big) \\ &\quad = \sum_{k=1}^{\eta} J_k\Big(x_k^{(0\sim\mu_k-1)}(t), r_k^{(0\sim\mu_k-1)}(t), T_P, \rho, m, t\Big), \end{aligned} \tag{5}$$

where

$$J_k(\cdot) = \frac{1}{2}\int_0^{T_p} \left\| \left(\hat{x}_k^{(0\sim\mu_k-1)}|_{k=1\sim\eta}(t+\tau) - \hat{r}_k^{(0\sim\mu_k-1)}(t+\tau)\right)\right\|^2 \mathrm{d}\tau, \tag{6}$$

and ρ, m and T_P are predictive parameters, which represent the predictive order, the control order and the length of the predictive period, respectively. For $k = 1, 2, \cdots, \eta$, $r_k^{(0\sim\mu_k-1)}(t)$, $r_k \in \mathbb{R}^{r_k}$ are the prescribed reference signal generated by the known reference inputs $v_{rk}(t) \in \mathbb{R}^{r_k}$, given as follows:

$$r_k^{(\mu_k)}(t) = v_{rk}(t), \ k = 1, 2, \cdots, \eta, \tag{7}$$

and $\hat{x}_k^{(0\sim\mu_k-1)}|_{k=1\sim\eta}(t+\tau)$ and $\hat{r}_k^{(0\sim\mu_k-1)}(t+\tau)$ are the predictive states and the reference signals characterized in a moving time period frame, given as follows

$$\hat{x}_k^{(0\sim\mu_k-1)}|_{k=1\sim\eta}(t+\tau) \triangleq x_k^{(0\sim\mu_k-1)}(t) + \tau\dot{x}_k^{(0\sim\mu_k-1)}(t) + \cdots + \frac{1}{\rho!}\tau^{\rho}\left(x_k^{(0\sim\mu_k-1)}(t)\right)^{(\rho)}, \tag{8}$$

and

$$\hat{r}_k^{(0\sim\mu_k-1)}(t+\tau) \triangleq r_k^{(0\sim\mu_k-1)}(t) + \tau\dot{r}_k^{(0\sim\mu_k-1)}(t) + \cdots + \frac{1}{\rho!}\tau^{\rho}\left(r_k^{(0\sim\mu_k-1)}(t)\right)^{(\rho)}. \tag{9}$$

To be explicit statement of the problem, we introduce the following assumptions.

Assumption 2. The state $x_k^{(0\sim\mu_k-1)}|_{k=1\sim\eta}$ is available.

Assumption 3. The reference signal $r_k^{(0\sim\mu_k-1)}|_{k=1\sim\eta}$ and the state $x_k^{(0\sim\mu_k-1)}|_{k=1\sim\eta}$ are sufficiently differentiable.

Assumption 4. The predictive order is no less than the control order, that is, $\rho \geq m$.

Then the problem of this paper can be stated as follows:

Problem 1. For the continuous-time mix-order nonlinear FA system (3) satisfying Assumptions 1–4, find an optimal controller of the following form

$$u(t) = -B^{-1}(\cdot)\Big(f(\cdot) - v_k|_{k=1\sim\eta}\Big(x_k^{(0\sim\mu_k-1)}(t), r_k^{(0\sim\mu_k-1)}(t), T_P, \rho, m, t\Big)\Big), \tag{10}$$

where $v_k(\cdot) \in \mathbb{R}^{r_k}$, $k = 1, 2, \cdots, \eta$, are a series of MPC optimization controllers with respect to the corresponding states, reference signals and predictive parameters such that the receding-horizon performance index (5) is minimized.

Remark 2. For Assumption 2, we concentrate on the state tracking optimization problem of a deterministic system, it is a conventional assumption that the state $x_k^{(0\sim\mu_k-1)}|_{k=1\sim\eta}$ is available. According to the characterized predictive states and the reference signals in (8) and (9), which involves multiple derivatives of states and reference signals, so Assumption 3 is a necessary condition. And Assumption 3 is made in most of nonlinear control theory [45].

Remark 3. For Assumption 4, in the forward moving time period frame, the predictive state can be regarded as a Taylor expansion as (4). However, it can be observed that the order of the controls derivative is not greater than the states in the differential equations of system (1). Nonetheless, we take multi-order derivatives of the differential equations into the Taylor expansion, it is impossible that the order of the control derivative is higher than states in the expression of the predictive state. Then the corresponding control order defined in Definition 1 should always no larger than the predictive order.

3. HOFA system approach for MPC

In this section, we concentrate on the nonlinear MPC optimization problem based on HOFA system approaches. The proposed scheme of HOFA-MPC is derived into three parts.

3.1. Model conversion

Taking the controller (10) into the system (3), one have

$$x_k^{(\mu_k)}|_{k=1\sim\eta}(t) = v_k|_{k=1\sim\eta}(t).$$

From the above equation, a series of decouped HOFA systems can be directly obtained as

$$x_k^{(\mu_k)}(t) = v_k(t), \ \ k = 1, 2, \cdots, \eta. \tag{11}$$

Further, the above linear systems can be intuitively described into the canonical form as follows:

$$\dot{x}_k^{(0\sim\mu_k-1)}(t) = A_k x_k^{(0\sim\mu_k-1)}(t) + B_k v_k(t), \ \ k = 1, 2, \cdots, \eta, \tag{12}$$

where

$$\begin{cases} A_k = \Phi\left(0_{0\sim\mu_k-1}\right) \\ B_k = \begin{bmatrix} 0 \\ \vdots \\ 0 \\ I_{r_k} \end{bmatrix}. \end{cases} \tag{13}$$

Similarly, it follows from (7) that the equivalent reference system can be written as

$$\dot{r}_k^{(0\sim\mu_k-1)}(t) = A_k r_k^{(0\sim\mu_k-1)}(t) + B_k v_{rk}(t),\ \ k = 1, 2, \cdots, \eta. \tag{14}$$

Denote the tracking error as

$$e_k^{(0\sim\mu_k-1)}|_{k=1\sim\eta}(t) = x_k^{(0\sim\mu_k-1)}|_{k=1\sim\eta}(t) - r_k^{(0\sim\mu_k-1)}|_{k=1\sim\eta}(t), \tag{15}$$

then the tracking error system can be formulated as

$$e_k^{(0\sim\mu_k-1)}|_{k=1\sim\eta}(t) = A e_k^{(0\sim\mu_k-1)}(t) + B v_e(t),$$

where

$$\begin{cases} A = \text{blockdiag}(A_k,\ \ k = 1, 2, \cdots, \eta) \\ B = \text{blockdiag}(B_k,\ \ k = 1, 2, \cdots, \eta), \end{cases}$$

and

$$v_e(t) = v(t) - v_r(t).$$

It follows from (15) that each $e_k^{(0\sim\mu_k-1)}$ can be decoupled, and we have

$$e_k^{(0\sim\mu_k-1)}(t) = x_k^{(0\sim\mu_k-1)}(t) - r_k^{(0\sim\mu_k-1)}(t),\ \ k = 1, 2, \cdots, \eta. \tag{16}$$

Moreover, each decoupled tracking error subsystem can be given as

$$\dot{e}_k^{(0\sim\mu_k-1)}(t) = A_k e_k^{(0\sim\mu_k-1)}(t) + B_k v_{ek}(t),\ \ k = 1, 2, \cdots, \eta, \tag{17}$$

where

$$v_{ek}(t) = v_k(t) - v_{rk}(t). \tag{18}$$

3.2. Predictive information construction

It can be observed from (10) that the controller transformation mapping can be regarded a differential homeomorphism from u to v for all $x_k^{(0\sim\mu_k-1)}$, $r_k^{(0\sim\mu_k-1)}$ and predictive parameters. Then the control order of u and v are equal, and the control order of the decoupled input v_{ek} and v are also equal.

According to the tracking error subsystem (17), the multi-order derivatives of the tracking error $e_k^{(0\sim\mu_k-1)}$ with the control order m and the predictive order ρ is given as follows:

$$\left(e_k^{(0\sim\mu_k-1)}(t)\right)^{(i)} = \begin{cases} A_k^i e_k^{(0\sim\mu_k-1)}(t) + A_k^{i-1} B_k v_{ek}(t) + \cdots + B_k v_{ek}^{(i)}(t),\ \ 1 \le i \le m \\ A_k^i e_k^{(0\sim\mu_k-1)}(t) + A_k^{i-1} B_k v_{ek}(t) + \cdots + A_k^{i-m} B_k v_{ek}^{(m-1)}(t),\ \ m < i \le \rho. \end{cases}$$

Further, the decoupling predictive tracking errors in each moving time period frame can be rewritten as

$$\hat{e}_k^{(0\sim\mu_k-1)}(t+\tau) = T_{0\sim\rho}\bar{A}_k e_k^{(0\sim\mu_k-1)}(t) + T_{1\sim\rho}\bar{B}_k v_{ek}^{(0\sim m-1)}(t),\ \ k = 1, 2, \cdots, \eta, \tag{19}$$

where

$$\begin{cases} \bar{A}_k = \begin{bmatrix} I_{\mu_k r_k} \\ A_k \\ \vdots \\ A_k^{\rho} \end{bmatrix} \\ \bar{B}_k = \begin{bmatrix} B_k & 0 & \cdots & 0 \\ A_k B_k & B_k & \cdots & 0 \\ \vdots & \vdots & \ddots & \vdots \\ A_k^{m-1} B_k & A_k^{m-2} B_k & \cdots & B_k \\ \vdots & \vdots & \vdots & \vdots \\ A_k^{\rho-1} B_k & A_k^{\rho-2} B_k & \cdots & A_k^{\rho-m} B_k \end{bmatrix}, \end{cases} \tag{20}$$

and

$$\begin{cases} T_k^{0\sim\rho} = \begin{bmatrix} I_{\mu_k r_k} & \tau I_{\mu_k r_k} & \cdots & \dfrac{1}{\rho!}\tau^{\rho} I_{\mu_k r_k} \end{bmatrix} \\ T_k^{1\sim\rho} = \begin{bmatrix} \tau I_{\mu_k r_k} & \dfrac{1}{2!}\tau^2 I_{\mu_k r_k} & \cdots & \dfrac{1}{\rho!}\tau^{\rho} I_{\mu_k r_k} \end{bmatrix}. \end{cases}$$

Similarly, vectors of the reference signal $r_k^{(0\sim\mu_k-1)}$ in each moving time period frame can be expressed as

$$\hat{r}_k^{(0\sim\mu_k-1)}(t+\tau) = T_k^{0\sim\rho} r_k^{(0\sim\mu_k-1)}(t), \ \ k = 1, 2, \cdots, \eta. \tag{21}$$

3.3. Nonlinear optimization decomposition

Taking (19) and (21) into the receding-period performance index (5), the optimal index can be converted as follows

$$J(\cdot) = \frac{1}{2}\sum_{k=1}^{\eta} \int_0^{Tp} \left\| \Lambda_k e_k^{(0\sim\mu_k-1)}(t) + \digamma_k v_{ek}^{(0\sim m-1)}(t) \right\|^2 \mathrm{d}\tau, \tag{22}$$

where

$$\begin{cases} \Lambda_k = T_k^{0\sim\rho} \bar{A}_k \\ \digamma_k = T_k^{1\sim\rho} \bar{B}_k. \end{cases} \tag{23}$$

Then the nonlinear optimization problem in Problem 1 is transformed into a linear convex one. Moreover, it can be decomposed into a series of independent linear minimization problems as follows:

$$\min_{v_{ek}} J_k(\cdot) = \frac{1}{2}\int_0^{T_p} \left\| \Lambda_k e_k^{(0\sim\mu_k-1)}(t) + \digamma_k v_{ek}^{(0\sim m-1)}(t) \right\|^2 \mathrm{d}\tau, \ \ k = 1, 2, \cdots, \eta. \tag{24}$$

By taking the derivative of J_k along $v_{ek}^{(0\sim m-1)}$, we have

$$v_{ek}^{(0\sim m-1)}(t) = -\int_0^{Tp} \left(\digamma_k^{\mathrm{T}} \digamma_k\right)^{-1} \digamma_k^{\mathrm{T}} \Lambda_k \mathrm{d}\tau, \ \ k = 1, 2, \cdots, \eta. \tag{25}$$

Taking the second derivative of J_k along $v_{ek}^{(0\sim m-1)}$, one have

$$\frac{\partial^2 J_k}{\partial^2 v_{ek}^{(0\sim m-1)}} = \int_0^{Tp} \Lambda_k^{\mathrm{T}} \Lambda_k \mathrm{d}\tau > 0,$$

then the vector of controllers (25) are the corresponding minimum vector of solutions for (24).

Since the integration of τ in the index (24) are only related to $T_k^{1\sim\rho}$ and $T_k^{0\sim\rho}$, then $v_{ek}^{(0\sim m-1)}$ can be further formulated with (23) as follows

$$v_{ek}^{(0\sim m-1)}(t) = -\left(\bar{B}_k^{\mathrm{T}} \Gamma_k^1 \bar{B}_k\right)^{-1} \bar{B}_k^{\mathrm{T}} \Gamma_k^2 \bar{A}_k e_k^{(0\sim\mu_k-1)}(t),$$

where Γ_k^1 and Γ_k^2 can be calculated as follows

$$\begin{aligned} \Gamma_k^1 &= \int_0^{Tp} \left(T_k^{1\sim\rho}\right)^{\mathrm{T}} T_k^{1\sim\rho} \mathrm{d}\tau \\ &= \mathrm{blockdiag}\left(T_p C_k\right) \mathrm{block}\left\{ \frac{1}{(i+j+1)} I_{\mu_k r_k}, {}^{i=1\sim\rho}_{j=1\sim\rho} \right\} C_k, \end{aligned} \tag{26}$$

$$\begin{aligned} \Gamma_k^2 &= \int_0^{Tp} \left(T_k^{1\sim\rho}\right)^{\mathrm{T}} T_k^{0\sim\rho} \mathrm{d}\tau \\ &= \mathrm{blockdiag}\left(T_p C_k\right) \mathrm{block}\left\{ \frac{1}{(i+j+1)} I_{\mu_k r_k}, {}^{i=1\sim\rho}_{j=0\sim\rho} \right\} \mathrm{blockdiag}\left(I_{\mu_k r_k}, C_k\right), \end{aligned} \tag{27}$$

and

$$C_k = \mathrm{blockdiag}\left(\frac{T_p^j}{j!} I_{\mu_k r_k}, \ \ j = 1 \sim \rho \right).$$

Thus, the optimal solution can be arranged as

$$v_e(t) = -K e_k^{(0\sim\mu_k-1)}|_{k=1\sim\eta}(t), \tag{28}$$

where

$$\begin{cases} K = \mathrm{blockdiag}(\kappa_k, \ \ k = 1, 2, \cdots, \eta) \\ \kappa_k = \Gamma_k \bar{A}_k \\ \Gamma_k = \overbrace{\left[I_{\mu_k r_k} \quad 0 \quad \cdots \quad 0 \right]}^{m} \left(\bar{B}_k^{\mathrm{T}} \Gamma_k^1 \bar{B}_k\right)^{-1} \bar{B}_k^{\mathrm{T}} \Gamma_k^2. \end{cases}$$

Building upon the foregoing analysis, we can conclude the following theorem.

Theorem 1. *Suppose that Assumptions 1–4 are met for the nonlinear system* (1)*, then the solution to Problem* 1 *is given as*

$$u = -B^{-1}(\cdot)\left[f(\cdot) + K\left(x_k^{(0\sim\mu_k-1)}|_{k=1\sim\eta}(t) - r_k^{(0\sim\mu_k-1)}|_{k=1\sim\eta}(t) \right) - v_r(t) \right], \tag{29}$$

where

$$\begin{cases} K = \mathrm{blockdiag}(\kappa_k, \ \ k = 1, 2, \cdots, \eta) \\ \kappa_k = \overbrace{\left[I_{r_k} \quad 0 \quad \cdots \quad 0 \right]}^{m} \left(\bar{B}_k^{\mathrm{T}} \Gamma_k^1 \bar{B}_k\right)^{-1} \bar{B}_k^{\mathrm{T}} \Gamma_k^2 \bar{A}_k, \end{cases} \tag{30}$$

and $\bar{A}_k$, $\bar{B}_k$ Γ_k^1 *and* Γ_k^2 *are given in* (20), (26) *and* (27).

Remark 4. It is difficult to obtain an analytical solution in nonlinear optimization problems, but this is achieved in this paper. Due to the full-actuation property of the system, we directly eliminate the complex nonlinearies which include time-varying and time-delay, and decouple the nonlinear optimization problems into a series of linear optimization problems. For the linear optimization problem, it is easily obtained an explicit analytical solution.

Remark 5. Note that the feedback gain K is a constant calculated by off-line optimization, which depended on the numbers and dimensions of states in system (1) and predictive parameters. And the optimal controller (29) has well-known feed-forward and feedback structures. To be specific, $Kr_k^{(0\sim\mu_k-1)}|_{k=1\sim\eta}(t)+v_r(t)$ is a feed-forward compensation term based on the tracking signals and reference input vector, and $Kx_k^{(0\sim\mu_k-1)}|_{k=1\sim\eta}$ is a typical state feedback item.

3.4. Stability analysis for closed-loop system

To facilitate the subsequent proof, we partition κ_k as

$$\kappa_k=\begin{bmatrix}\kappa_{k,1} & \kappa_{k,2} & \cdots & \kappa_{k,\mu_k}\end{bmatrix},\ \kappa_{k,i}\in\mathbb{R}^{r_k\times r_k}, \tag{31}$$

and denotes as $\kappa_{k,1\sim\mu_k}$.

Taking the controller (30) into (17), the closed-loop tracking error systems can be obtained as

$$\dot{e}_k^{(0\sim\mu_k-1)}|_{k=1\sim\eta}(t)=A_c e_k^{(0\sim\mu_k-1)}|_{k=1\sim\eta}, \tag{32}$$

where

$$A_c=\text{blockdiag}\{A_{ck},\ k=1,2,\cdots,\eta\},$$

and

$$A_{ck}=A_k-B_k\kappa_k. \tag{33}$$

And the closed-loop tracking error subsystems can be also obtained as

$$\dot{e}_k^{(0\sim\mu_k-1)}(t)=A_{ck}e_k^{(0\sim\mu_k-1)},\ k=1,2,\cdots,\eta. \tag{34}$$

Theorem 2. *Suppose that Assumptions 1–4 are met for the nonlinear HOFA system* (1)*, then* (1) *the closed-loop error dynamics system* (32) *is asymptotically stable if the predictive parameters are appropriately chosen such that the matrices* $\Phi_k\left(\kappa_{k,1\sim\mu_k}\right)$, $k=1,2,\cdots,\eta$, *are Hurwitz;* (2) *if one of the following conditions*

$$\begin{cases}\rho-m>r_k\\ m\geq r_k\\ \gamma=\chi,\end{cases}$$

holds, then the stability of the closed-loop tracking error system (32) *is only depended on m and* T_p.

Proof. From the partition of κ_k in (31), we have

$$A_{ck}=\begin{bmatrix}0 & I_{r_k} & \cdots & 0\\ 0 & 0 & \ddots & 0\\ \vdots & \vdots & \cdots & I_{r_k}\\ -\kappa_{k,1} & -\kappa_{k,2} & \cdots & -\kappa_{k,\mu_k}\end{bmatrix}.$$

And A_{ck} can be presented as $\Phi_k(\kappa_{k,1\sim\mu_k})$. If the predictive parameters are appropriately chosen such that $\Phi_k(\kappa_{k,1\sim\mu_k})$, $k=1,2,\cdots,\eta$, are a series of Hurwitz matrices, then the closed-loop tracking error subsystems (34) are asymptotically stable, and the closed-loop tracking error system (32) is asymptotically stable.

Further, we analyze the relationship between the stability of closed-loop tracking error system with predictive parameters. Taking (26) and (27) into the second equation of (30), we have

$$\begin{aligned}\left(\bar{B}_k^{\mathrm{T}}\Gamma_k^1\bar{B}_k\right)^{-1}\bar{B}_k^{\mathrm{T}}\Gamma_k^2\bar{A}_k = &\left(\bar{B}_k^{\mathrm{T}}\mathrm{block}\left\{\frac{1}{(i+j+1)}I_{\mu_k r_k}{}_{j=1\sim\rho}^{i=1\sim\rho}\right\}\bar{B}_k\right)^{-1}\\ &\times\bar{B}_k^{\mathrm{T}}\left(\mathrm{block}\left\{\frac{i!T_p^{-i}}{(i+j+1)}I_{\mu_k r_k}{}_{j=0}^{i=1\sim\rho}\right\}\right.\\ &\left.+\ \mathrm{block}\left\{\frac{1}{(i+j+1)}I_{\mu_k r_k}{}_{j=1\sim\rho}^{i=1\sim\rho}\right\}\bar{A}_{k,1\sim\rho}\right),\end{aligned}\tag{35}$$

then κ_k, $k=1,2,\cdots,\eta$, are related to the predictive parameters ρ, m and T_p. So, we can conclude the first conclusion. For the first condition and the second condition in the second conclusion, according to the first equation of (20), when $m>r_k$ or $\rho-m>r_k$, we have

$$A_k^{\rho-m-1}=A_k^m=0_{\mu_k r_k},$$

and

$$\bar{A}_k=\begin{bmatrix}\bar{A}_k'\\0\\\vdots\\0\end{bmatrix},\quad \bar{B}_k=\begin{bmatrix}\bar{B}_k'\\0\\\vdots\\0\end{bmatrix},\tag{36}$$

where $\bar{A}_k'\in\mathbb{R}^{m\mu_k r_k\times\mu_k r_k}$ and $\bar{B}_k'\in\mathbb{R}^{m\mu_k r_k\times m r_k}$ are given as follows:

$$\bar{A}_k'=\begin{bmatrix}I_{\mu_k r_k}\\A_k\\\vdots\\A_k^{m-1}\end{bmatrix},\quad \bar{B}_k'=\begin{bmatrix}B_k&0&\cdots&0\\*&B_k&\cdots&0\\\vdots&\vdots&\ddots&\vdots\\*&*&\cdots&B_k\end{bmatrix}.\tag{37}$$

Further the Eq. (35) can be simplified as

$$\begin{aligned}&\left(\bar{B}_k^{\mathrm{T}}\Gamma_k^1\bar{B}_k\right)^{-1}\bar{B}_k^{\mathrm{T}}\Gamma_k^2\bar{A}_k\\&=\left(\left(\bar{B}_k'\right)^{\mathrm{T}}\mathrm{block}\left\{\frac{1}{(i+j+1)}I_{\mu_k r_k}{}_{j=1\sim m}^{i=1\sim m}\right\}\bar{B}_k'\right)^{-1}\\&\quad\times\left(\bar{B}_k'\right)^{\mathrm{T}}\left(\mathrm{block}\left\{\frac{i!T_p^{-i}}{(i+j+1)}I_{\mu_k r_k}{}_{j=0}^{i=1\sim m}\right\}+\mathrm{block}\left\{\frac{1}{(i+j+1)}I_{\mu_k r_k}{}_{j=1\sim m}^{i=1\sim m}\right\}\bar{A}_k'\right),\end{aligned}\tag{38}$$

then combing the second equation of (30) we can conclude that κ_k is only depended with m and T_p. For the third condition in the second conclusion, when $\gamma=\chi$, it follows from (2) that $\mu_k=1$, $k=1,2,\cdots,\eta$. Then system (1) is a first-order nonlinear system, and A_k, B_k are given as follows

$$A_k=0,\quad B_k=I_{r_k},$$

and $\bar{A}'_k$ and $\bar{B}'_k$ in (37) can be written as

$$\bar{A}'_k = I_{r_k}, \ \bar{B}'_k = I_{mr_k}.$$

Then the Eq. (35) can be further simplified as

$$\left(\bar{B}_k^{\mathrm{T}}\Gamma_k^1\bar{B}_k\right)^{-1}\bar{B}_k^{\mathrm{T}}\Gamma_k^2\bar{A}_k = \left(\mathrm{block}\left\{\frac{1}{(i+j+1)}I_{\mu_k r_k}, {}^{i=1\sim m}_{j=1\sim m}\right\}\right)^{-1} \times \left(\mathrm{block}\left\{\frac{i!T_p^{-i}}{(i+j+1)}I_{\mu_k r_k}, {}^{i=1\sim m}_{j=0}\right\} + \mathrm{block}\left\{\frac{1}{(i+j+1)}I_{\mu_k r_k}, {}^{i=1\sim m}_{j=1\sim m}\right\}\right),$$

then $\kappa_k \in \mathbb{R}^{r_k \times r_k}$ is the matrix only related to m and T_p. Thus, the whole proof is then completed. □

Remark 6. In conventional MPC nonlinear methods without constraints, they linearize the nonlinear system by feedback linearization, firstly. But this first-step process is quite complex based on state-space models, which require finding the appropriate output and performing multiple calculations of the Lie algebra. Not to mention that this process will become more complicated if there exist vectors of time-delay and time varying. Intuitively, different from feedback linearization, the HOFA system approaches are more flexible and easier. Whether dealing with state-space models or original high-order models, they can eliminate complex nonlinearities and decouple variables through simple elimination operations from control variables. It has been proved that all models linearized by feedback linearization can be transformed into HOFA systems, and HOFA system approaches can also solve problems that cannot be solved by feedback linearization [8].

4. Examples of under-actuated systems and simulation

In this section, to thoroughly verify the performance of the proposed approach, two examples of under-actuated systems are conducted from model conversions and simulation, respectively. And in each example, we have introduced four cases for quantitative comparative analysis.

In order to assess the performance of the proposed scheme, we compare the efficiency under the three algorithms: the proposed method in this paper as Algorithm 1, the method proposed in [13] as Algorithm 2, and the nonlinear MPC in [19] as Algorithm 3.

And the following performance evaluation indicators are used: $T_{2\%}$ is the setting time or the recovery time under the disturbance within 2% steady errors, $\xi_{\max}$ and $\eta_{\max}$ are the absolute maximum values of the states, and MAE presents the mean absolute error of input.

4.1. Example 1: A numerical example

Consider the first-order continuous-time plant mentioned in [46]

$$\begin{cases} \dot{\eta} = \eta^2 + \xi \\ \dot{\xi} = u, \end{cases} \tag{39}$$

where η, $\xi \in \mathbb{R}$ are states, $u \in \mathbb{R}$ is the control input. This simple nonlinear system is under-actuated in mathematical sense. From the first equation of (39), one have

$$\xi = \dot{\eta} - \eta^2. \tag{40}$$

Table 1
Performance indexes for stabilization.

Parameter	$T_{2\%}-\eta$	$T_{2\%}-\xi$	$\eta_{\max}$	$\xi_{\max}$	MAE
Algorithm 1	4.1	3.6	0	0.2476	0.4588
Algorithm 2	4	3.8	0.011	0.2658	0.4118
Algorithm 3	6.7	6.2	0.0067	2.852	1.365

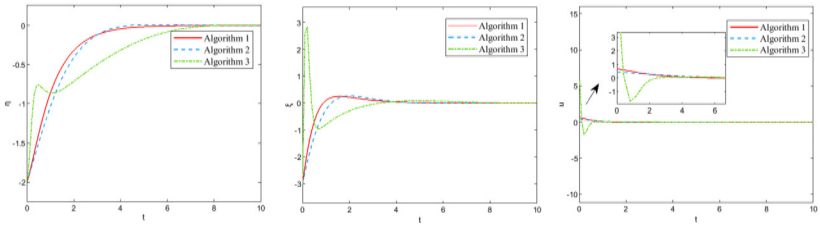

Fig. 1. Simulation results of Algorithm 1–3. The responses of η, ξ and u are shown from left to left. Red solid line: Algorithm 1; blue dashed line: Algorithm 2; green dotted-dashed line: Algorithm 3. (For interpretation of the references to colour in this figure legend, the reader is referred to the web version of this article.)

Taking the first-order derivatives of ξ, and substituting it into the second equation of (39), then a second-order FA system can be obtained as follows:

$$\ddot{\eta} = 2\eta\dot{\eta} + u. \tag{41}$$

It can see that the first-order under-actuated system (39) in mathematical sense has been equivalently converted into a second-order nonlinear FA system, which is the case of $k, r_k = 1$ and $\mu_k = 2$ in system (1). And from the state conversion in (40), the state ξ is redundant for the system (39), which only depends on the vector of the state $\eta^{(0\sim1)}$. Then in the new FA system (41), variable η and $\dot{\eta}$ can be directly controlled by the controller, which means that η and ξ can be directly controlled, but it cannot be realized in the original system (39).

Case 1. Stabilization.

The reference signals are $\eta_r(t) = \xi_r(t) = 0$, and the initial states are $\eta(0) = -2$ and $\xi(0) = -3$. Selecting the parameters as $\rho = 10$, $m = 5$ and $T_p = 4$, such that $\Phi_1(\kappa_{1\sim2})$ is Hurwize. The results are shown in Table 1 and Fig. 1.

From Table 1 and Fig. 1, it can be observed that compared with Algorithm 3, Algorithm 1 and Algorithm 2 based on HOFA system approaches have significant advantages in states responses, states overshoot and the input energy. In terms of stabilization performance, the comparisons between Algorithm 1 and Algorithm 2 are quite slight.

Case 2. States recovery under the disturbance.

We add a pulse disturbance with the value of 3 lasting 1s at 5s on the input. The simulation results are shown in Table 2 and Fig. 2.

From the Table 2 and Fig. 2, it is clearly seen that regardless of performance indicators or the speed of state recovery, the performance of Algorithm 1 is the most significant when the controller has to cope with a pulse disturbance. Therefore, we have that the proposed Algorithm 1 possesses the strongest states recovery capability than Algorithm 2 and Algorithm 3.

Table 2
Performance indexes for states recovery.

Parameter	$T_{2\%} - \eta$	$T_{2\%} - \xi$	$\eta_{\max}$	$\xi_{\max}$	MAE
Algorithm 1	5	4	0.1508	0.4081	0.0477
Algorithm 2	5.7	5.9	0.3285	0.602	0.0685
Algorithm 3	6.9	4.4	0.958	2.915	0.7138

Table 3
Performance indexes for different T_p.

T_P	$T_{2\%} - \eta$	$T_{2\%} - \xi$	$\eta_{\max}$	$\xi_{\max}$	MAE
1	4.1	3.6	0.0012	0.1349	11.33
3	4	3.8	0.0001	0.2458	8.193
5	6.7	6.2	0.0001	0.2421	5.907

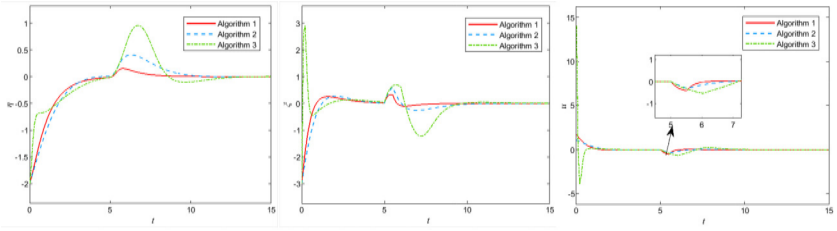

Fig. 2. Simulation results of Algorithm 1–3 with the disturbance. The responses of η, ξ and u are shown from left to right. Red solid line: Algorithm 1; blue dashed line: Algorithm 2; green dotted-dashed line: Algorithm 3. (For interpretation of the references to colour in this figure legend, the reader is referred to the web version of this article.)

At the same time, we have tested the different ρ with fixed m and T_P satisfying $\rho > m + r_1$. There are no changes in the responses of the system, so we omit this part of the results. Thus, it also verifies the conclusion in Theorem 2 that when $\rho > m + r_1$, the dynamical of the closed-loop system is only related to T_P and m. Then the following two cases are given as follows.

Case 3. $\rho = 10$, $m = 5$ and $T_P = 1,\ 3,\ 5$.

When $\rho = 10$, $m = 5$ and $T_P = 1,\ 3,\ 5$, the corresponding $\Phi_1(\kappa_{1,1\sim 2})$ is Hurwize, and the predictive parameters satisfies the first condition in the second conclusion of Theorem 2. The results are shown in Table 3 and Fig. 3.

According to Table 3 and Fig. 3, it can be seen that the state response is not very sensitive to T_P, but MAE is sensitive to T_P.The control energy can be reduced by increasing the predictive period. This is easy to understand that the longer predictive period is, more prediction information we have, we can adjust the control input timely to minimize the optimal index with less control energy. It can be also confirmed from the Eq. (38), as T_P increases, the corresponding κ_1 increases.

Case 4. Let $T_P = 1$, $\rho = 10$ and $m = 1,\ 2,\ 3$.

The above selected predictive parameters make the corresponding $\Phi_1(\kappa_{1,1\sim 2})$ are Hurwize. The results are shown in Table 4 and Fig. 4.

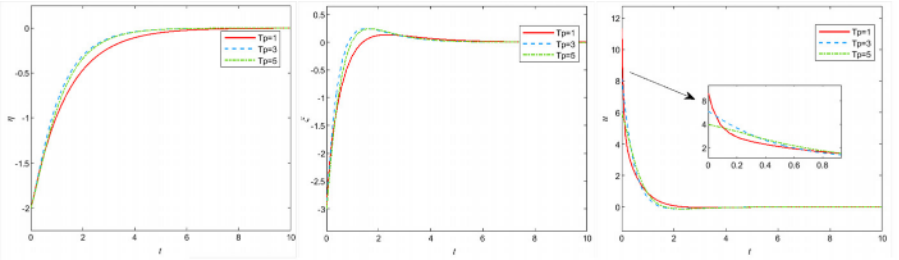

Fig. 3. Responses of different T_P. The responses of η, ξ and u from left to right. Red solid line: $T_P = 1$; blue dashed line: $T_P = 3$; green dotted-dashed line: $T_P = 5$. (For interpretation of the references to colour in this figure legend, the reader is referred to the web version of this article.)

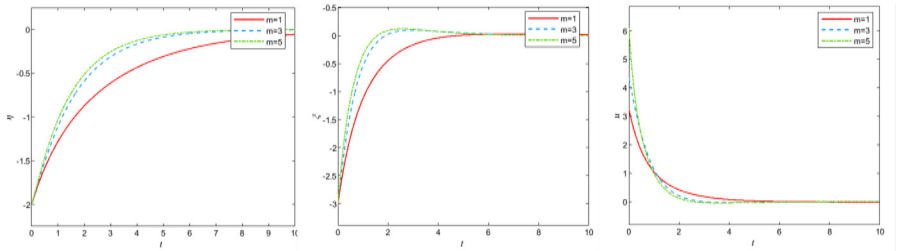

Fig. 4. Responses of different m. The responses of η, ξ and u from left to right. Red solid line: $m = 1$; blue dashed line: $m = 3$; green dotted-dashed line: $m = 5$. (For interpretation of the references to colour in this figure legend, the reader is referred to the web version of this article.)

Table 4
Performance indexes for different m.

m	$T_{2\%} - \eta$	$T_{2\%} - \xi$	$\eta_{\max}$	$\xi_{\max}$	MAE
1	10	5.692	0.04	0.02825	0.4922
3	6.214	5.251	0.0037	0.1	0.5698
5	5.631	4.285	0.0019	0.121	0.6475

The setting time can be reduced by increasing the control order, but the more control energy is required for prediction. And according to Fig. 4 and Table 4, it can be seen that the state response has a high sensitivity to m.

4.2. Example 2: A benchmark under-actuated system

4.2.1. Model conversion

Consider the robotic system jointed with a direct current motor [47,48]

$$\begin{cases} J_1\ddot{q}_1(t) + F_1\dot{q}_1(t) + K\left(q_1(t) - \dfrac{q_2(t)}{N}\right) + mgd\cos q_1(t) = 0 \\ J_2\ddot{q}_2(t) + F_2\dot{q}_2(t) - \dfrac{K}{N}\left(q_1(t) - \dfrac{q_2(t)}{N}\right) = K_t i(t) \\ L\dot{i}(t) + Ri(t) + K_b\dot{q}_2(t) = u(t), \end{cases} \tag{42}$$

where $q_1,\ q_2 \in \mathbb{R}$ are the angular positions of the link and the motor shaft, i and u are the armature current and the voltage. The constants J_1 and J_2 are the inertias, F_1 and F_2 are the viscous friction constants, K is the spring constant, K_t is the torque constant, K_b is the back-emf constant, R and L are the armature resistance and the inductance, m is the link mass, d is the position of the link's center of gravity, N is the gear ratio, and g is the acceleration of gravity. For convenience, variable t will be omitted in the following procedures.

And from the first equation of the above model, we have

$$q_2 = \frac{N}{K}(J_1\ddot{q}_1 + F_1\dot{q}_1 + mgd\cos q_1) + q_1, \tag{43}$$

taking the first-order and second-order derivative of q_2, and substituting them into the second equation of the model (42), one can obtain

$$\begin{aligned} i =& \frac{J_1^2 N}{KK_t}q_1^{(4)} + \frac{J_1 N(F_1+F_2)}{KK_t}q_1^{(3)} + \left(\frac{F_1F_2N}{KK_t} - \frac{J_1mgdN}{KK_t}\sin(q_1) + \frac{J_1N}{K_t} + \frac{J_1}{NK_t}\right)\ddot{q}_1 \\ & - \frac{J_1mgdN}{KK_t}\cos(q_1)\dot{q}_1^2 + \left(-\frac{mgdNF_2}{KK_t}\sin(q_1) + \frac{NF_2}{K_t} + \frac{F_1}{NK_t}\right)\dot{q}_1 + \frac{mgdN}{N^2K_t}\cos(q_1). \end{aligned} \tag{44}$$

Further taking the first-order derivative of the above equation, and substituting it into the third equation of the model (42), a fifth-order FA system can be obtained as

$$q_1^{(5)} + f\left(q_1^{(0\sim4)}\right) = B\left(q_1^{(0\sim4)}\right)u, \tag{45}$$

where

$$\begin{cases} f\left(q_1^{(0\sim4)}\right) = & a_1q_1^{(4)} + \left(a_2 - \dfrac{mgd}{J_1}\sin(q_1)\right)q_1^{(3)} - \dfrac{3mgd}{J_1}\cos(q_1)\dot{q}_1\ddot{q}_1 \\ & +(a_3 - a_4\sin(q_1))\ddot{q}_1 + \dfrac{mgd}{J_1}\sin(q_1)\dot{q}_1^3 - a_4\dot{q}_1^2 \\ & -(a_5\sin(q_1) - a_6)\dot{q}_1 - a_7q_1 + a_8\cos(q_1) \\ B\left(q_1^{(0\sim4)}\right) = & \dfrac{KK_t}{J_1J_2LN}, \end{cases}$$

and

$$\begin{cases} a_1 = \dfrac{L(F_1J_2 + F_2J_1) + J_1J_2R}{J_1J_2L} \\ a_2 = \dfrac{R(F_1J_2 + F_2J_1) + F_1F_2L + J_1K_bK_t}{J_1J_2L} + \dfrac{J_1K + J_2KN}{J_1J_2N^2} \\ a_3 = \dfrac{J_1KR + F_1KL}{J_1J_2LN^2} + \dfrac{F_2LK + K_bK_tF_1N + J_2RK + F_1F_2NR}{J_1J_2LN} \\ a_4 = mgd\dfrac{J_2R + F_2L}{J_1J_2L} \\ a_5 = mgd\dfrac{N^2(K_tK_b + RF_2) + KL}{J_1J_2LN^2} \\ a_6 = \dfrac{N^2(KK_tK_b + KRF_2) + KRNF_1 - K^2L(N-1)}{J_1J_2LN^3} \\ a_7 = \dfrac{K^2R(N-1)}{J_1J_2LN^3} \\ a_8 = \dfrac{KRmgd}{J_1J_2LN^2}. \end{cases}$$

Table 5
Performance indexes for tracking.

Parameter	$T_{2\%} - q_{e_1}$	$q_{e_1 \max}$	MAE
Algorithm 1	5.9	0.0044	0.0258
Algorithm 2	6.2	0.0078	0.9999
Algorithm 3	11.4	0.0507	0.5863

From the above operation of model conversion, a mix-order under-actuated system is converted into a fifth-order FA system, which is the case of $k = 1$ and $\mu_k = 5$ in system (1). It follows from (43) and (7) that the redundant variables $q_2^{(0\sim1)}$ and i are depended on $q_1^{(0\sim3)}$ and $q_1^{(0\sim4)}$, that is, the state vector $q_1^{(0\sim4)}$ can determine all states in the system, directly. Therefore, for subsequent state tracking control, we only need to ensure the state tracking of $q_1^{(0\sim4)}$.

4.3. Simulation results

Following [49], we choose $F_1 = J_1 = K = F_2 = N = R = L = K_b = K_t = 1$, $g = 10$, $m = 1/2$, and $d = 1/5$. The initial states are given as: $q_1(0) = -0.2$, $\dot{q}_1(0) = 0.1$, $q_2(0) = -0.1$, $\dot{q}_2(0) = 0.1$, $i(0) = 0.1$.

In order to test the effectiveness of the proposed methods and the influence of the predictive parameters, we conduct four cases as follows.

Case 5. Tracking control.

The reference signals are sine-like waves generated by the following system

$$\dot{q}_r^{(4)} = A_1 q_r^{(0\sim4)} + B_1 v_r,$$

where

$$A_1 = \begin{bmatrix} 0 & 1 & 0 & 0 & 0 \\ 0 & 0 & 1 & 0 & 0 \\ 0 & 0 & 0 & 1 & 0 \\ 0 & 0 & 0 & 0 & 1 \\ 0 & 0 & 0 & 0 & 0 \end{bmatrix}, \quad B_1 = \begin{bmatrix} 0 \\ 0 \\ 0 \\ 0 \\ 1 \end{bmatrix},$$

and v_r is the known reference input given as

$$v_r = \begin{bmatrix} -1 & -3 & -4 & -4 & -3 \end{bmatrix} q_r^{(0\sim4)}.$$

Selecting the parameters as $\rho = 15$, $m = 9$ and $T_p = 8$, such that the $\Phi_1(\kappa_{1,1\sim5})$ is Hurwize. Limited by the length of the paper, we only give the results about state q_1 as Table 5 and Fig. 5.

From Table 5 and Fig. 5, a similar conclusion is obtained from the corresponding case in Example 1 that Algorithm 1 has the fastest state response, smallest error overshoot, and it is especially superior in terms of input energy than Algorithm 2 and Algorithm 3.

Case 6. Tracking recovery under the disturbance.

The selection of predictive parameters is the same as in the above case. We add a pulse disturbance with the value of 1 lasting 0.5s at 8s. The results are shown in Table 6 and Fig. 6.

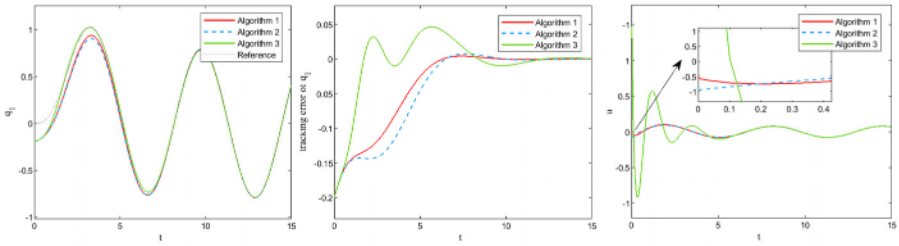

Fig. 5. Simulation results of Algorithm 1–3. The tracking responses of q_1, tracking error q_{e_1} and u are shown from left to right. Red solid line: Algorithm 1; blue dashed line: Algorithm 2; green dotted-dashed line: Algorithm 3; purple dotted lines: reference single. (For interpretation of the references to colour in this figure legend, the reader is referred to the web version of this article.)

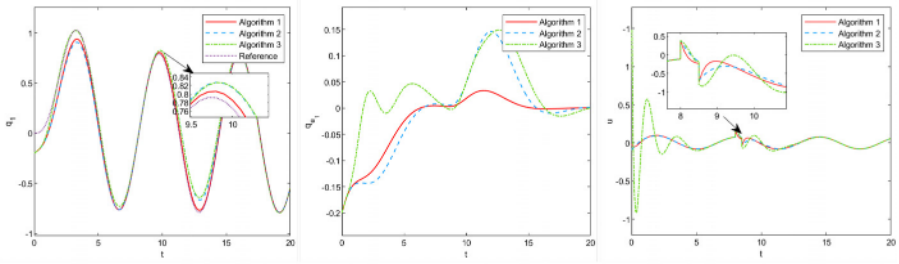

Fig. 6. Simulation results of Algorithm 1–3 with disturbance. The tracking responses of q_1, tracking error q_{e_1} and u are shown from left to right. Red solid line: Algorithm 1; blue dashed line: Algorithm 2; green dotted-dashed line: Algorithm 3; purple dotted lines: reference single. (For interpretation of the references to colour in this figure legend, the reader is referred to the web version of this article.)

Table 6
Performance indexes for tracking recovery.

Parameter	$T_{2\%} - q_{e_1}$	$q_{e_1 \max}$	MAE
Algorithm 1	6.2	0.0333	0.0143
Algorithm 2	7.5	0.146	0.0317
Algorithm 3	8.3	0.1664	0.4357

In this case, the advantages of Algorithm 1 are more significant than the above case. The responses of states are more smooth and faster, the control energy is significantly less compared with Algorithm 2 and Algorithm 3.

Case 7. $\rho = 15$, $m = 9$ and $T_P = 3,\ 5,\ 8$.

The selected predictive parameters keep the corresponding $\Phi_1\left(\kappa_{1,1\sim5}\right)$ is Hurwize. The system dynamical performance with the different predictive period are shown in Table 7 and Fig. 7.

It can be seen that as the increase of the predictive period, the dynamical tracking performance of the system is slightly improved, but less control force is needed. Because the longer predictive period can indicate more information about the controller's influence on states, and the system only needs less control force. But the responses of the system are not sensitive to T_P.

Table 7
Performance indexes for differen T_p.

T_P	$T_{2\%} - q_{e_1}$	$q_{e_1\,\max}$	MAE
3	8.91	0.0101	0.0844
5	7.71	0.0042	0.0727
8	5.91	0.0044	0.0381

Table 8
Performance indexes for differen m.

m	$T_{2\%} - q_{e_1}$	$q_{e_1\,\max}$	MAE
5	9.51	0.0073	0.011
7	6.71	0.0041	0.0122
9	5.91	0.0037	0.0524

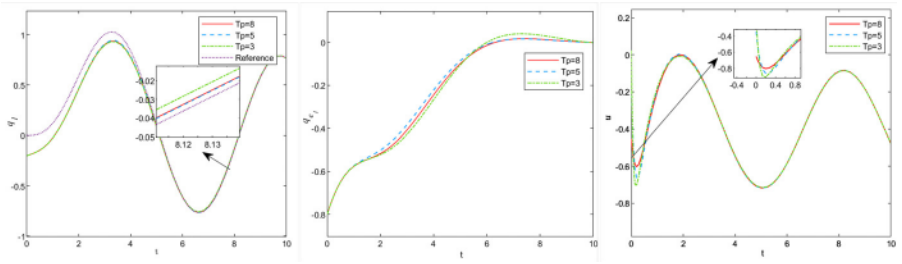

Fig. 7. Responses of different T_P. The tracking responses of q_1, tracking error q_{e_1} and u are shown from left to right. Red solid line: $T_P = 8$; blue dashed line: $T_P = 5$; green dotted-dashed line: $T_P = 3$; purple dotted lines: reference single. (For interpretation of the references to colour in this figure legend, the reader is referred to the web version of this article.)

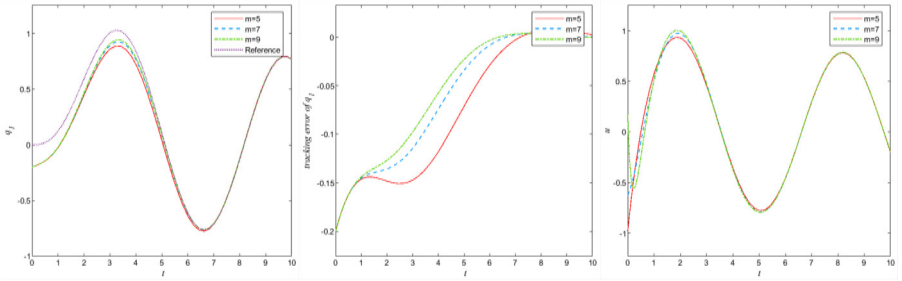

Fig. 8. Responses of different m. The tracking responses of q_1, tracking error q_{e_1} and u are shown from left to right. Red solid line: $m = 8$; blue dashed line: $m = 7$; green dotted-dashed line: $m = 9$; purple dotted lines: reference single. (For interpretation of the references to colour in this figure legend, the reader is referred to the web version of this article.)

Case 8. $\rho = 15,\ T_P = 8$ and $m = 5,\ 7,\ 9$.

The selected predictive parameters keep the corresponding $\Phi_1(\kappa_{1\sim5})$ is Hurwize. And the dynamical performance is shown in the Table 8 and the Fig. 8.

According to Table 8 and Fig. 8, we can draw a similar conclusion in the corresponding case of Example 1. The tracking response has a high sensitivity to m. The response speed of

the system can be accelerated, and the overshoot of the tracking error can be reduced as the control order increases, but the more control energy is required.

5. Conclusion

In this paper, we investigate a new MPC tracking optimization based on HOFA system approaches, which is applicable to a broad class of nonlinear systems with the strongly nonlinear, mix-order, even time-varying and time-delay factors. Under the full-actuation condition, the nonlinear optimization problem is converted into a series of easy-solve convex linear ones, and a smooth and explicit analytical controller can be obtained directly. The effectiveness of the proposed method is demonstrated by the under-actuated system of a numerical example and a benchmark practical application.

The proposed method can be ulteriorly generalized. In terms of the system form, the method in this paper can be generalized to the case of discrete-time systems, time-delay systems, stochastic systems, etc. From the construction of the optimal performance index, we will take constraints of the system, the control energy and the prescribed performance into consideration in the future work. Particularly, the constraints MPC for sub-FA systems based on HOFA systems approaches is already one of the main contents in our follow-up research based on this paper.

Declaration of Competing Interest

The authors declare that they have no known competing financial interests or personal relationships that could have appeared to influence the work reported in this paper.

References

[1] G. Duan, High-order fully actuated system approaches: part I. models and basic procedure, Int. J. Syst. Sci. 52 (2) (2021) 422–435.
[2] G. Duan, High-order fully actuated system approaches: part II. generalized strict-feedback systems, Int. J. Syst. Sci. 52 (3) (2021) 437–454.
[3] F. Xiao, L. Chen, Attitude control of spherical liquid-filled spacecraft based on high-order fully actuated system approaches, J. Syst Sci. Complex. 35 (2) (2022) 471–480.
[4] M. Cai, X. He, D. Zhou, Fault-tolerant tracking control for nonlinear observer-extended high-order fully-actuated systems, J. Franklin. Inst. 360 (1) (2023) 136–153.
[5] G. Liu, Coordination of networked nonlinear multi-agents using a high-order fully actuated predictive control strategy, IEEE/CAA J. Autom. Sin. 9 (4) (2022) 615–623.
[6] T. Zhao, G. Duan, Fully actuated system approach to attitude control of flexible spacecraft with nonlinear time-varying inertia, Sci. China Inform. Sci. 65 (11) (2022) 1–15.
[7] H. Sun, L. Huang, L. He, Research on the trajectory tracking control of a 6-DOF manipulator based on fully-actuated system models, J. Syst Sci. Complex. 35 (2) (2022) 641–659.
[8] G. Duan, Stabilization via fully actuated system approach: a case study, J. Syst Sci. Complex. 35 (3) (2022) 731–747.
[9] G. Duan, Brockett'S first example: an FAS approach treatment, J. Syst Sci. Complex. 35 (2) (2022) 441–456.
[10] G. Duan, Brockett'S second example: an FAS approach treatment, J. Syst Sci. Complex. 10.1007/s11424-022-2282-2
[11] G. Duan, High-order fully actuated system approaches: part V. robust adaptive control, Int. J. Syst. Sci. 52 (10) (2021) 2129–2143.
[12] G. Duan, High-order fully-actuated system approaches: part VI. disturbance attenuation and decoupling, Int. J. Syst. Sci. 52 (10) (2021) 2161–2181.

[13] G. Duan, High-order fully actuated system approaches: part VIII. optimal control with application in spacecraft attitude stabilisation, Int. J. Syst. Sci. 53 (1) (2022) 54–73.
[14] G. Duan, High-order fully-actuated system approaches: part IX. generalised PID control and model reference tracking, Int. J. Syst. Sci. 53 (3) (2022) 652–674.
[15] G. Duan, Discrete-time delay systems: part 2. sub-fully actuated case, Sci. China Inform. Sci. 65 (9) (2022) 1–15.
[16] G. Duan, Fully actuated system approaches for continuous-time delay systems: part 1. systems with state delays only, Sci. China Inform. Sci. 66 (1) (2023) 1–30.
[17] G. Duan, Fully actuated system approaches for continuous-time delay systems: part 2. systems with input delays, Sci. China Inform. Sci. 66 (2) (2023) 122201.
[18] G. Duan, Robust stabilization of time-varying nonlinear systems with time-varying delays: a fully actuated system approach, IEEE Trans. Cybern. 10.1109/TCYB.2022.3217317
[19] Y. Igarashi, M. Yamakita, J. Ng, H.H. Asada, MPC Performances for Nonlinear Systems Using Several Linearization Models, in: 2020 American Control Conference (ACC), IEEE, 2020, pp. 2426–2431.
[20] A. Lashab, D. Sera, J. Guerrero, A dual-discrete model predictive control-based MPPT for PV systems, IEEE Trans. Power Electron. 34 (10) (2019) 9686–9697.
[21] H. Zhang, L. Du, J. Shen, Hybrid MPC system for platoon based cooperative lane change control using machine learning aided distributed optimization, Transport. Res. B-Meth. 159 (2022) 104–142.
[22] D. Zhao, D. Liu, L. Liu, Distributed MPC algorithm with row-stochastic weight matrix over non-ideal time–varying directed communication, IET Control Theory A. 16 (18) (2022) 1860–1872.
[23] C. Shen, Y. Shi, Distributed implementation of nonlinear model predictive control for AUV trajectory tracking, Automatica 115 (2020) 108863.
[24] M. Hu, C. Li, Y. Bian, H. Zhang, Z. Qin, B. Xu, Fuel economy-oriented vehicle platoon control using economic model predictive control, IEEE Trans. Intell. Transp. Syst. 23 (11) (2022) 20836–20849.
[25] D. Tavernini, M. Metzler, P. Gruber, A. Sorniotti, Explicit nonlinear model predictive control for electric vehicle traction control, IEEE Trans. Control Syst. Technol. 27 (4) (2018) 1438–1451.
[26] H. Xie, L. Dai, Y. Lu, Y. Xia, Disturbance rejection MPC framework for input-affine nonlinear systems, IEEE Trans. Automat. Contr. 67 (12) (2021) 6595–6610.
[27] Y. Xu, Y. Yuan, D. Zhou, The composite-disturbance-observer based stochastic model predictive control for spacecrafts under multi-source disturbances, J. Franklin. Inst. 358 (15) (2021) 7603–7627.
[28] M. Bujarbaruah, U. Rosolia, Y. Stürz, X. Zhang, F. Borrelli, Robust mpc for LPV systems via a novel optimization-based constraint tightening, Automatica 143 (2022) 110459.
[29] J. Köhler, P. Kötting, R. Soloperto, F. Allgöwer, M.A. Müller, A robust adaptive model predictive control framework for nonlinear uncertain systems, Int. J. Robust Nonlinear Control 31 (18) (2021) 8725–8749.
[30] P. He, J. Wen, V. Stojanovic, F. Liu, X. Luan, Finite-time control of discrete-time semi-markov jump linear systems: a self-triggered mpc approach, J. Franklin. Inst. 359 (13) (2022) 6939–6957.
[31] R. Wan, S. Li, Y. Zheng, Model predictive control for nonlinear systems with time-varying dynamics and guaranteed lyapunov stability, Int. J. Robust Nonlinear Control 31 (2) (2021) 509–523.
[32] A. Li, J. Sun, Stability of nonlinear system under distributed lyapunov-based economic model predictive control with time-delay, ISA Trans. 99 (2020) 148–153.
[33] B. Karg, S. Lucia, Efficient representation and approximation of model predictive control laws via deep learning, IEEE Trans. Cybern. 50 (9) (2020) 3866–3878.
[34] L. Hewing, K. Wabersich, M. Menner, M.N. Zeilinger, Learning-based model predictive control: toward safe learning in control, Annu. Rev. Contr. Robot. 3 (2020) 269–296.
[35] A. Wischnewski, T. Herrmann, F. Werner, B. Lohmann, A tube-MPC approach to autonomous multi-vehicle racing on high-speed ovals, IEEE Trans. Intell. Veh. 8 (1) (2023) 368–378.
[36] V. Djordjevic, V. Stojanovic, H. Tao, X. Song, S. He, W. Gao, Data-driven control of hydraulic servo actuator based on adaptive dynamic programming, Discrete Cont. Dyn-A. 15 (7) (2022) 1633.
[37] R. Chai, A. Tsourdos, H. Gao, Y. Xia, S. Chai, Dual-loop tube-based robust model predictive attitude tracking control for spacecraft with system constraints, and additive disturbances, IEEE Trans. Ind. Electron. 69 (4) (2021) 4022–4033.
[38] A. Parra, D. Tavernini, P. Gruber, A. Sorniotti, A. Zubizarreta, J. Pérez, On nonlinear model predictive control for energy-efficient torque-vectoring, IEEE Trans. Veh. Technol. 70 (1) (2020) 173–188.
[39] D. Pereira, F. Lopes, E. Watanabe, Nonlinear model predictive control for the energy management of fuel cell hybrid electric vehicles in real time, IEEE Trans. Ind. Electron. 68 (4) (2020) 3213–3223.

[40] M. Schwenzer, M. Ay, T. Bergs, D. Abel, Review on model predictive control: an engineering perspective, Int. J. Adv. Manuf. Tech. 117 (5) (2021) 1327–1349.
[41] M. Morato, J. Normey-Rico, O. Sename, Model predictive control design for linear parameter varying systems: a survey, Annu. Rev. Control 49 (2020) 64–80.
[42] X. Song, P. Sun, S. Song, V. Stojanovic, Event-driven NN adaptive fixed-time control for nonlinear systems with guaranteed performance, J. Franklin. Inst. 359 (9) (2022) 4138–4159.
[43] Z. Li, L. Wu, Y. Xu, S. Moazeni, Z. Tang, Multi-stage real-time operation of a multi-energy microgrid with electrical and thermal energy storage assets: a data-driven MPC-ADP approach, IEEE Trans. Smart Grid 13 (1) (2021) 213–226.
[44] W. Chen, D. Ballance, P. Gawthrop, Optimal control of nonlinear systems: a predictive control approach, Automatica 39 (4) (2003) 633–641.
[45] H. Nijmeijer, A. Schaft, Nonlinear dynamical control systems, Springer, 1990.
[46] D. Nesic, A. Teel, Backstepping on the Euler Approximate Model for Stabilization of Sampled-data Nonlinear Systems, in: Proceedings of the 40th IEEE Conference on Decision and Control (Cat. No. 01CH37228), IEEE, 2001, pp. 1737–1742.
[47] Z. Zhao, Z. Jiang, Finite-time output feedback stabilization of lower-triangular nonlinear systems, Automatica 96 (2018) 259–269.
[48] M. Krstic, P. Kokotovic, I. Kanellakopoulos, Nonlinear and adaptive control design, John Wiley & Sons, Inc., 1995.
[49] X. Xie, N. Duan, Output tracking of high-order stochastic nonlinear systems with application to benchmark mechanical system, IEEE Trans. Automat. Contr. 55 (5) (2010) 1197–1202.